THE JOURNAL OF BIOLOGICAL CHEMISTRY VOL. 285, NO. 4, pp. 2653–2664, January 22, 2010

Rhesus Glycoprotein P2 (Rhp2) Is a Novel Member of the Rh Family of Ammonia Transporters Highly Expressed in Shark Kidney*[S]

Received for publication, August 10, 2009, and in revised form, November 17, 2009 Published, JBC Papers in Press, November 19, 2009, DOI 10.1074/jbc.M109.052068

Tsutomu Nakada[‡1], Connie M. Westhoff[§¶2], Yoko Yamaguchi[‖], Susumu Hyodo[‖], Xiaojin Li[¶], Takayuki Muro[‡], Akira Kato[‡], Nobuhiro Nakamura[‡], and Shigehisa Hirose[‡3]

From the [‡]Department of Biological Sciences, Tokyo Institute of Technology, Yokohama 226-8501, Japan, the [§]Department of Pathology and Laboratory Medicine, University of Pennsylvania, Philadelphia, Pennsylvania 19104, the [¶] American Red Cross, Philadelphia, Pennsylvania 19130, and the [‖]Laboratory of Physiology, Ocean Research Institute, University of Tokyo, Tokyo 164-8639, Japan

Rhesus (Rh) glycoproteins are a family of membrane proteins capable of transporting ammonia. We isolated the full-length cDNA of a novel Rh glycoprotein, Rhp2, from a kidney cDNA library from the banded hound shark, *Triakis scyllium*. Molecular cloning and characterization indicated that Rhp2 consists of 476 amino acid residues and has 12 putative transmembrane spans, consistent with the structure of other family members. The shark *Rhp2* gene was found to consist of only one coding exon. Northern blotting and *in situ* hybridization revealed that Rhp2 mRNA is exclusively expressed in the renal tubules of the sinus zone but not in the bundle zone and renal corpuscles. Immunohistochemical staining with a specific antiserum showed that Rhp2 is localized in the basolateral membranes of renal tubule cells. Double fluorescence labeling with phalloidin or labeling of the Na^+/K^+-ATPase further narrowed the location to the second and fourth loops in the sinus zone. Vacuolar type H^+-ATPase was localized in apical membranes of the Rhp2-expressing tubule cells. Quantitative real-time PCR analysis and Western blotting showed that expression of Rhp2 was increased in response to elevation of environmental salinity. Functional analysis using the *Xenopus* oocyte expression system showed that Rhp2 has transport activity for methylammonium, an analog of ammonia. This transport activity was inhibited by NH_4Cl but not trimethylamine-*N*-oxide and urea. These results suggested that Rhp2 is involved in ammonia reabsorption in the kidney of the elasmobranch group of cartilaginous fish comprising the sharks and rays.

Members of the Rhesus (Rh)[4] glycoprotein family are membrane proteins present in a broad range of eukaryotes including insects, sea squirts, fish, birds, amphibians, and mammals. Six clusters of the Rh family (RhAG, RhBG, RhCG, RH30, Rhp1, and Rhp2 (p is for primitive)) have been defined by an extensive phylogenetic analysis (1). Among the family members, RhAG, RhBG, and RhCG are present in most vertebrates and are known to be capable of transporting ammonia[5] and methylammonium (2–9). The Rhp1 members are present in several invertebrates including aquatic crab *Carcinus maenas* (10), sea squirt *Ciona intestinalis*, and the fruit fly *Drosophila melanogaster* (1). Furthermore, Rhp1 was shown to be essential for embryonic development and hypodermal function in *Caenorhabditis elegans* (11). In contrast, *Rhp2* genes were identified in genomes of non-mammalian vertebrates only by data base mining, and the function and localizations of their protein products (Rhp2) have not been characterized in any species. We previously isolated the cDNA fragments of two Rhp2s (synonym for Rhag-like1 and Rhag-like2) from puffer fish; however, no mRNA transcripts were observed in any tissues examined (12).

Rhag, Rhbg, Rhcg1, and Rhcg2 are expressed in the gill of puffer fish, where they excrete ammonia to eliminate nitrogenous waste (12). Moreover, Rh glycoproteins of rainbow trout (13–16), killifish (17), and zebrafish (18–20) have been characterized and were expressed in the tissues that are implicated in ammonia secretion. These observations strongly suggested that Rh glycoproteins are involved in ammonia excretion in teleost fish. In contrast, Rh glycoproteins of the elasmobranch fishes, which include sharks and rays, have not yet been identified. Nitrogen metabolism in the elasmobranch fishes differs greatly from the teleost fishes. Elasmobranch fish utilize ammonia to produce urea rather than directly excreting

* This work was supported by Grants-in-aid for Scientific Research 14104002 and 18059010 (to S. H.) and 18-5667 (to T. N.) from the Ministry of Education, Culture, Sport, Science and Technology of Japan (MEXT), the Japan Society for the Promotion of Science Research Fellowships for Young Scientists, and the 21st Century and Global Centers of Excellence Program of MEXT.

[S] The on-line version of this article (available at http://www.jbc.org) contains supplemental Table 1 and Fig. 1.

The nucleotide sequence(s) reported in this paper has been submitted to the DDBJ/GenBank™/EBI Data Bank with accession number(s) AB287007.

[1] Present address: T. Nakada, Dept. of Molecular Pharmacology, Shinshu University School of Medicine, Nagano 390-8621, Japan.

[2] To whom correspondence may be addressed: 700 Spring Garden St., Philadelphia, PA, 19130. Tel.: 215-451-4920; Fax: 215-451-4925; E-mail: westhoffc@usa.redcross.org.

[3] To whom correspondence may be addressed: 4259-B19 Nagatsuta-cho, Midori-ku, Yokohama-shi, Kanagawa-ken, 226-8501 Japan. Tel.: 81-45-924-5726; Fax: 81-45-924-5824; E-mail: shirose@bio.titech.ac.jp.

[4] The abbreviations used are: Rh, Rhesus; PBS, phosphate-buffered saline; TMAO, trimethylamine-*N*-oxide; RACE, rapid amplifications of cDNA ends; DIG, digoxigenin; UTR, untranslated region; MA, methylammonium; NKCC, Na^+-K^+-$2Cl^-$ cotransporter; V-ATPase, vacuolar-type H^+-ATPase; TRITC, tetramethylrhodamine isothiocyanate; MOPS, 4-morpholinepropanesulfonic acid.

[5] Ammonia exists in aqueous solutions in two molecular forms, NH_3 and NH_4^+, that are in equilibrium with each other. In this paper, the term "ammonia" refers to the combination of both forms. The term "ammonium" specifically refers to the molecular species NH_4^+. When referring to NH_3, we specifically state "NH_3."

ammonia from the gill. Moreover, urea is retained by renal reabsorption to maintain body fluid osmolality. The difference in ammonia metabolism between teleosts and elasmobranches led us to hypothesize that the Rh glycoproteins in each have distinct physiological roles. Thus, we attempted isolation of Rh glycoprotein cDNAs from hound shark using a degenerate PCR technique and characterization of their protein products.

In this study we identified a novel Rh glycoprotein from Japanese banded hound shark, *Triakis scyllium*. Phylogenetic analysis revealed that this novel Rh glycoprotein positions in the Rhp2 cluster. Northern blot analysis showed strong expression of Rhp2 exclusively in the kidney. *In situ* hybridization and immunohistochemistry showed that Rhp2 is localized in the basolateral membrane of renal tubule cells in the sinus zone. Furthermore, functional analysis in *Xenopus* oocytes showed that shark Rhp2 transports methylammonium, an analog of ammonia. This transport activity was inhibited by the addition of NH_4Cl but not trimethylamine-*N*-oxide (TMAO), urea, or tetraethylammonium chloride and had similar kinetic properties as the other Rh glycoprotein family members. These data suggested that Rhp2 is involved in ammonia transport in the kidney of elasmobranch fishes.

EXPERIMENTAL PROCEDURES

Animals—Japanese banded hound shark, *T. scyllium*, of both sexes (0.75–1.7 kg) were collected in Koajiro Bay, near the Misaki Marine Biological Station, University of Tokyo. They were kept with daily feeding of squid in a 4-kl round tank with running seawater (~12 °C) under a natural photoperiod for at least 1 week before experiments as previously described (21). For tissue sampling, fish were anesthetized in 0.002% (w/v) 3-aminobenzoic acid ethyl ester (Sigma). After decapitation, tissues were dissected and frozen quickly in liquid nitrogen. To examine the effects of environmental salinity on expression of Rhp2 mRNA, hound sharks were transferred to diluted (60%) or concentrated (130%) seawater as previously described (22). The animal protocols and procedures were approved by the Institutional Animal Care and Use Committees of Tokyo Institute of Technology and the University of Tokyo and conform to the American Physiological Society's "Guiding Principles in the Care and Use of Laboratory Animals" (23).

RNA Isolation and Molecular Cloning—Total RNA was isolated from tissues by acid guanidinium thiocyanate-phenol-chloroform extraction with Isogen (Nippon Gene, Tokyo, Japan). Tissues were homogenized in Isogen (1 g of tissue/10 ml of Isogen) using a Polytron tissue homogenizer followed by chloroform extraction, isopropanol precipitation, and 70% ethanol washing of precipitated RNA. The RNA obtained was dissolved in diethyl pyrocarbonate-treated water, and its concentration was measured spectrophotometrically at 260 nm.

A fragment of tsRhp2 cDNA was isolated by degenerate reverse transcription-PCR from shark kidney RNA. The PCR product was subcloned into pBluescript II SK(−) and sequenced with ABI PRISM 310 or 3130 (Applied Biosystems, Foster City, CA). This clone was used as a probe for Northern blot analysis of tsRhp2 (ts stands for *T. scyllium*). Full-length cDNA of tsRhp2 was obtained by 5′-rapid amplification of cDNA ends (RACE), 3′-RACE, and reverse transcription-PCR with RLM-RACE kit (Ambion, Austin, TX) as previously described (24). All primer sets used are listed in supplemental Table 1. For expression in mammalian cells, full-length cDNA of tsRhp2 was subcloned into the EcoRI/XhoI sites of pcDNA3.1(−) (Invitrogen) or the EcoRI/BamHI sites of p3×FLAG-CMV10 (Sigma). To prepare plasmid constructs for puffer fish Rh glycoproteins (fRhag, fRhbg, fRhcg1, and fRhcg2) (12), each full-length cDNA was subcloned into the NotI/BglII sites for p3×FLAG-CMV10.

Genomic PCR for isolation of the *tsRhp2* gene was performed with the Extract-N-Amp Tissue PCR kit (Sigma) according to the manufacturer's instructions. Genomic DNA was extracted from the skin of shark, and the target sequence was amplified using touchdown PCR. The Thermal cycler program was 1 min at 94 °C, 1 min at 70 °C, and 3 min at 72 °C for the first cycle, the annealing temperature was decreased by 1 °C/cycle until the annealing temperature was at 60 °C, and 30 more cycles were repeated at the same annealing temperature. The PCR product was directly sequenced with ABI PRISM 310 or 3130.

Data Base Search—To obtain the nucleotide sequences for phylogenetic analysis and estimation of exon/intron structures, BLAST searches were performed on the following databases: NCBI (blast.ncbi.nlm.nih.gov) for *Homo sapiens*, *Mus musculus*, and *Gallus gallus*; Ensembl for *Ornithorhynchus anatinus*, *Anolis carolinensis*, *Danio rerio*, *C. elegans*, *Xenopus tropicalis*, and *D. melanogaster*; Department of Energy Joint Genome Institute (www.jgi.doe.gov) for *Takifugu rubripes*, *Nitrosomonas europaea*, and *C. intestinalis*. Exon/intron organizations of the genes of interest were estimated using Wise2 and GENSCAN Web Server at the Massachusetts Institute of Technology.

Northern Blotting—Total RNA (10 μg/lane) from a pool of various tissues of hound shark was electrophoresed on formaldehyde-agarose (1%)-denaturing gels in MOPS running buffer (20 mM MOPS, pH 7.0, 8 mM acetate, 1 mM EDTA) and then transferred onto Hybond-N^+ nylon membranes (GE Healthcare) by capillary blotting. After transfer, membranes were baked for 2 h at 80 °C and prehybridized for 2 h at 65 °C in PerfectHyb hybridization solution (Toyobo, Osaka, Japan). The probes were labeled with [α-^{32}P]dCTP (3,000 Ci/mmol) with the use of a Ready-To-Go DNA labeling kit (GE Healthcare), and the unincorporated nucleotides were removed by passage through a Sephadex G-50 column (GE Healthcare). The membranes were then hybridized separately with each ^{32}P-labeled probe in the same buffer at 68 °C for 16 h. The blots were subsequently washed with increasingly stringent conditions (final wash, 1× SSC (0.15 M NaCl and 0.015 M sodium citrate) and 0.1% SDS for 30 min at 60 °C). Membranes were exposed to imaging plates (Fuji Film, Tokyo, Japan) in a cassette overnight. The results were analyzed using a Fuji BAS2000 Bio-image analyzer (Fuji Film). A probe for β-actin (25) was used as a control to verify loading and RNA integrity. Equal loading of RNA was further confirmed by ethidium bromide staining of 28 S and 18 S rRNA.

In Situ Hybridization—Kidney from anesthetized hound shark was fixed with 4% paraformaldehyde, embedded in paraffin, and sectioned (6 μm). The full-length tsRhp2 cDNA was used as the template for the preparation of digoxigenin (DIG)-labeled riboprobes. The DIG RNA labeling mix

(Roche Diagnostics) was used for synthesizing DIG-labeled sense and antisense probes. Alkaline phosphatase-conjugated anti-DIG antibody and nitro blue tetrazolium/5-bromo-4-chloro-3-indolyl phosphate substrates were used to visualize the signal followed by counterstaining with Kernechtrot (Muto Pure Chemicals, Tokyo, Japan). Images were acquired by using a BZ-9000 fluorescence microscope (Keyence, Osaka, Japan). For low magnification view, several images were acquired with a 20× objective lens and were joined seamlessly into a single image with the bundled software.

Antibody Production—A cDNA fragment encoding a part of the C terminus of tsRhp2 (amino acid residues 414–476) was subcloned into the BamHI/EcoRI site of the bacterial expression vector pGEX4T2 (GE Healthcare). The recombinant protein was purified with glutathione-Sepharose 4B (GE Healthcare) by following the manufacturer's instructions. Briefly, BL21 cells transformed with the expression vectors were used to inoculate 1.5 liters of LB broth containing 100 μg/ml ampicillin. The cultures were grown to an A_{600} of 0.5 at 37 °C, and protein expression was induced by adding isopropyl-1-thio-D-galactopyranoside to a final concentration of 0.3 mM for 4 h at 37 °C. The cells were harvested from the cultures by centrifugation and resuspended in 20 ml of phosphate-buffered saline (PBS) and then disrupted by freezing-thawing and sonication. After centrifugation (10,000 × *g* at 4 °C), supernatants were saved and purified with glutathione-Sepharose 4B (GE Healthcare). After purification, recombinant proteins were dialyzed against saline at 4 °C. Polyclonal antibodies were prepared in Japanese white rabbits by injecting ~200 μg of purified recombinant proteins emulsified with the adjuvant TiterMax Gold (CytRx, Norcross, GA) (1:1), intramuscularly at multiple sites. The rabbits were injected three times at 1-month intervals and bled 7 days after the third immunization.

Immunohistochemistry—Immunohistochemistry of kidney sections was performed as previously described with minor modifications (24). Kidneys of shark were fixed with 4% paraformaldehyde in PBS at 4 °C for 2 h. After incubation in PBS containing 20% sucrose for 16 h at 4 °C, specimens were frozen in Tissue Tek OCT compound on a cryostat holder. Sections (6 μm) were prepared in a cryostat at −20 °C, mounted on 3-aminopropyltriethoxysilane-coated glass slides, and air-dried for 1 h. After washing with PBS, sections were first incubated in PBS with 0.1% Triton X-100 for 10 min and incubated for 1 h at room temperature with 2.5% normal goat serum or 5% fetal bovine serum. After blocking, the sections were reacted with anti-tsRhp2 antiserum (1:2000) overnight at 4 °C. Sections were then washed with PBS and treated with Alexa Fluor 488-conjugated anti-rabbit IgG (1:1000, Invitrogen) and Hoechst 33342 (100 ng/ml, Invitrogen) for 1 h at room temperature. Preimmune serum and preabsorbed antiserum were used for negative controls. The preabsorbed antiserum was prepared as follows. Rhp2 antiserum solution was incubated with excess antigen (a ratio of 1 μl of antiserum to 45 μg of antigen) at 4 °C for overnight and then centrifuged at 12,000 × *g* for 30 min to remove precipitates. The rabbit antiserum against the B subunit of vacuolar-type H^+-ATPase (V-ATPase) (1:1000) (26) was used to localized V-ATPase. To visualize the brush border of the proximal tubule, TRITC-phalloidin (0.1 μg/ml, Sigma) was also added into the secondary antibody solutions. The rat anti-Na^+/K^+-ATPase (1:1000) (25) and Cy3-conjugated anti-rat IgG (1:2000, Jackson ImmunoResearch) were used to localize Na^+/K^+-ATPase. Fluorescence images were acquired by using an Axiovert 200M epifluorescence microscope (Carl Zeiss, Thornwood, NY) equipped with an ApoTome optical sectioning device (Carl Zeiss), a BZ-9000 fluorescence microscope (Keyence), or an LSM 5 Exciter laser scanning microscope (Carl Zeiss).

Western Blotting—HEK293T cells were transiently transfected with each plasmid (pcDNA3.1 (Mock), p3×FLAG-CMV10 (Mock), pcDNA-Rhp2, p3×FLAG-Rhp2, p3×FLAG-fRhag, p3×FLAG-fRhbg, p3×FLAG-fRhcg1 or p3×FLAG-fRhcg2) using TransFectin Lipid reagent (Bio-Rad). Twenty-four hours after transfection the cells were harvested in PBS containing protease inhibitor mixture (BD Biosciences) with a cell scraper. The cells were subjected to three times of freezing-thawing to disrupt the plasma membrane. The membrane fractions were collected by centrifugation at 12,000 × *g* for 10 min. The resultant pellets were resuspended in solubilizing buffer (50 mM Tris-HCl, 10 mM EDTA, 1% Triton X-100, and protease inhibitor mixture, pH 7.5). After gentle rocking at 4 °C for 30 min, Triton X-100-soluble membrane fractions were obtained by centrifugation at 12,000 × *g* for 10 min. The crude membrane fractions from shark kidney and liver were isolated as follows. The tissue samples were homogenized with 5 volumes of homogenization buffer (50 mM Tris, 10 mM EDTA, and protease inhibitor mixture, pH 7.5) and then centrifuged at 600 × *g* for 5 min to remove debris. The supernatants were again centrifuged at 12,000 × *g* for 30 min, and resultant pellets were resuspended in solubilizing buffer. Triton X-100-soluble membrane fractions were obtained by the same procedures as those of HEK293T. For an experiment of Fig. 7*B*, kidney lysates were prepared as follows. The tissue samples were homogenized with radioimmune precipitation assay buffer (25 mM Tris, 150 mM NaCl, 0.1% SDS, 1% sodium deoxycholate, 1% Nonidet P-40, and protease inhibitor mixture, pH 7.6) and then rotated overnight at 4 °C to extract proteins. The samples were centrifuged at 12,000 × *g* for 15 min to remove debris, and the supernatants were used for subsequent analysis.

The protein concentrations of the samples were determined by the BCA protein assay kit (Thermo Fisher Scientific Inc., Rockford, IL). The yielded membrane fractions were treated with or without peptide *N*-glycosidase F (New England Biolabs, Beverly, MA) according to the manufacturer's instruction. 10 μg (HEK293T) or 20 μg (tissues) of the proteins were separated by 10% SDS-PAGE and electroblotted onto polyvinylidene difluoride membranes. Nonspecific binding was blocked with 5% nonfat skim milk in TBST (100 mM Tris-HCl, pH 7.5, 150 mM NaCl, and 0.1% Tween 20) for 1 h at room temperature. The membranes were incubated with anti-Rhp2 antiserum, preabsorbed antiserum (see the immunochemistry part under "Experimental Procedures" for preparation of the preabsorbed antiserum) (1:10,000), anti-α-tubulin (1:3,000, Sigma), or anti-FLAG M2 antibody (1:2,000, Sigma) overnight at 4 °C. After washing with TBST, membranes were then reacted with horseradish peroxidase-conjugated donkey anti-rabbit IgG

(1:10,000, Jackson ImmunoResearch) or horseradish peroxidase-conjugated donkey anti-mouse IgG (1:10,000, Jackson ImmunoResearch) for 1 h at room temperature. The bound secondary antibody was visualized by enhanced chemiluminescence detection using ECL-Plus reagents (BD Biosciences) according to the manufacturer's instructions.

Oocyte Injection and [^{14}C]Methylammonium Uptake Assay—Capped cRNA was synthesized with SP6 RNA polymerase using plasmid DNA containing the Rhp2 clone with mMessage mMachine (Ambion). Stage V and VI defolliculated oocytes were injected with 34 nl (1 ng/nl) of cRNA or water for controls and placed in individual wells in 96-well plates with 200 μl of SOS (100 mM NaCl, 2 mM KCl, 1.8 mM $CaCl_2$, 1 mM $MgCl_2$, 10 mM HEPES, pH 7.6) supplemented with 2.5 mM sodium pyruvate, and 100 μg/ml gentamicin at 16 °C. Radiolabeled methylammonium ($[^{14}C]CH_3NH_3^+$) (ICN, Irvine, CA) uptake was measured 3 days post-injection. Flux experiments were performed at room temperature as described previously (5, 8) by placing groups of six oocytes in 200 μl of low K^+ (0.2 mM) SOS uptake buffer containing 1 μCi/ml [^{14}C]methylammonium (MA) and unlabeled MA to a final concentration of 1.5 mM. For all experiments, radiotracer uptake was terminated by washing the oocytes several times with 1.2 ml of ice-cold unlabeled uptake buffer. Oocytes were solubilized in 200 μl of 5% SDS and analyzed for radioactivity in 5 ml of CytoScint (ICN) by liquid scintillation counting. Water-injected control oocytes were evaluated in parallel in all assays. Effects of TMAO (Wako Pure Chemicals, Osaka, Japan), urea, and NH_4Cl on MA uptakes were examined by the same method using groups of four oocytes in the presence or absence of the compounds in the uptake buffer. Kinetic data were analyzed with Igor software (WaveMetrics, Lake Oswego, OR). Initial uptake rates were determined from slopes of linear fits to uptake measured over short periods (7–15 min). Apparent EC_{50} (K_m) and V_{max} values were derived by fitting experimental data with a Michaelis-Menten or Hill equation using a nonlinear least-squares fitting algorithm.

Quantification of Rhp2 mRNA by Real-time PCR—Quantification of mRNA levels by real-time PCR was described in detail previously (27). To generate a standard curve for mRNA quantification, a partial cDNA fragment of hound shark Rhp2 was amplified by PCR from plasmid containing full-length Rhp2 cDNA. The preparation of glyceraldehyde-3-phosphate dehydrogenase as the internal control was performed as previously described (27). Total RNA was extracted from the kidney using Isogen (Nippon Gene) and treated with RNase-free DNase I (Takara, Kyoto, Japan) at 37 °C for 30 min to reduce contamination by genomic DNA. After inactivation of DNase, 5 μg of RNA was used as a template for reverse transcription using the SuperScript III First-Strand Synthesis System for reverse transcription-PCR (Invitrogen). Real-time PCR was performed with an ABI Prism 7900HT Sequence Detection system (Applied Biosystems). The PCR mixture (20 μl) contained Power SYBR Green PCR Master Mix (Applied Biosystems), 200 nM (Rhp2) or 100 nM (glyceraldehyde-3-phosphate dehydrogenase) forward and reverse primers, and standard cDNA (10^{-3}–10^{-7} ng/reaction) or 50 nl of reverse-transcribed cDNA samples. The intra- and interassay variations (n = 3) were 1.9 and 3.0%, respectively. The specificity of the method was confirmed by a dissociation analysis according to the instructions supplied by Applied Biosystems.

RESULTS

Molecular Properties of tsRhp2—To isolate cDNA clones coding for Rh glycoproteins, we carried out degenerate PCR using kidney and gill cDNAs of Japanese banded hound shark, *T. scyllium*. The degenerate primers were designed to target a highly conserved region between mammalian and teleost Rh glycoproteins in the predicted second and seventh transmembrane domains. An ~540-bp fragment was amplified and sequenced to confirm that the cDNA encodes a member of the Rh glycoprotein family. The complete coding sequence was obtained by 5′- and 3′-RACE and deposited in the DDBJ/EMBL/GenBank™ data base (accession no. AB287007). The isolated cDNA was ~1.6 kb long including 124 bp of 5′-untranslated region (UTR) and 67 bp of 3′-UTR. The coding region was predicted to encode a protein of 476 amino acid residues with a calculated molecular mass of 52 kDa (Fig. 1*A*). Like other members of the Rh glycoprotein family, hydrophobicity analysis of the protein predicted a membrane topology with 12 putative transmembrane spans and intracellular N and C termini (Fig. 1, *B* and *C*). The protein contains a putative protein kinase C phosphorylation site (Thr-461) and an *N*-glycosylation site (Asn-40) that is conserved in the first extracellular domain of all Rh glycoprotein family members (Fig. 1, *A* and *C*).

As expected, the amino acid sequence deduced from the isolated cDNA shares high identity with human RhAG (43.9%), RhBG (45.3%), RhCG (46.7%), *C. intestinalis* Rhp1 (40.5%), and *N. europaea* Rh protein (33.7%), indicating that the cDNA encodes a shark Rh glycoprotein. It has higher sequence identity with the predicted amino acid sequences of other members of the Rhp2 cluster such as those of zebrafish (55.2%), puffer fish (Rhp2a, 54.8%; Rhp2b, 55.2%), and frog (48.9%). Based on this fact and the phylogenetic analysis described below, we named the cloned shark Rh glycoprotein "tsRhp2" (ts for *T. scyllium*).

Phylogenetic Analysis and Gene Structure of Rhp2 Genes—We made a phylogenetic tree using the deduced amino acid sequence of the isolated cDNA and those of several Rh glycoproteins of other species. Amino acid sequences of bacteria (*N. europaea*), invertebrates (nematode, fruit fly, and sea squirt), mammals (human and platypus), teleost fish (puffer fish), reptile (green anole lizard), bird (chicken), and amphibian (western clawed frog) were used for the analysis. The shark tsRhp2 protein is positioned in the Rhp2 cluster defined by Huang *et al.* (1) (Fig. 2). The *Rhp2* genes are present in the genomes of most vertebrates except the human. Interestingly, the genomes of mouse and rat also lack the *Rhp2* gene, whereas that of platypus has the *Rhp2* gene (accession No. XP_001507563). In the platypus genomic data base, however, there is a gap in the nucleotide sequence corresponding to the C terminus of Rhp2; therefore, we used the partial sequence of 454 amino acid residues for the phylogenetic analysis. A partial cDNA sequence for Rhp2 was also found in the expressed sequence tag data base of chicken (GenBank™ accession no.

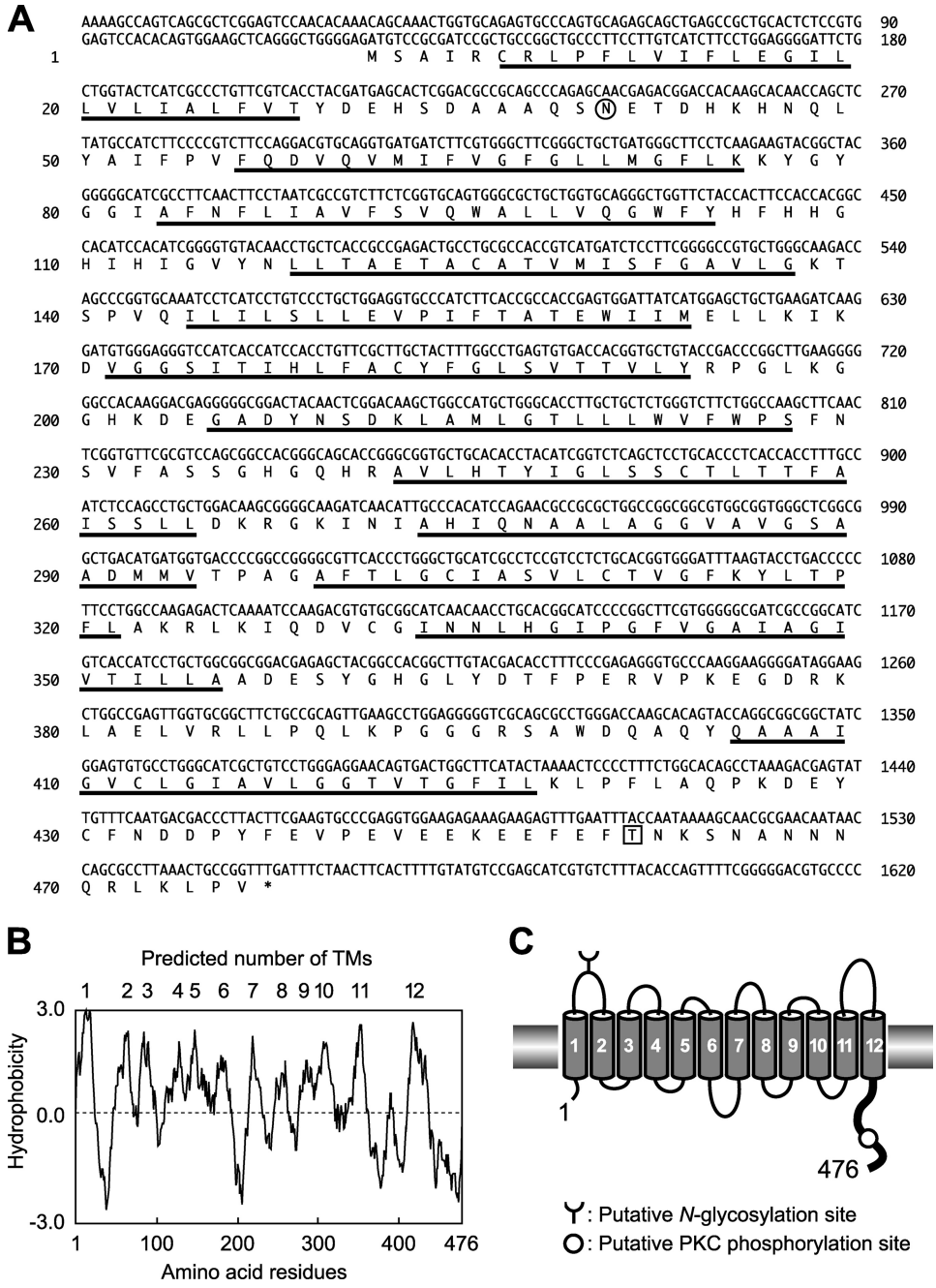

FIGURE 1. **Structural features of shark Rhp2.** *A*, nucleotide and deduced amino acid sequences of Rhp2 cDNA are shown. *Numbers on the left* refer to the first amino acid residue on the line, and *numbers on the right* refer to the last nucleotide on the line. The asterisk (*) indicates a stop codon. The *circled* and *squared* amino acid residues are potential *N*-glycosylation and protein kinase C phosphorylation sites, respectively. Twelve transmembrane-spanning regions predicted by hydrophobicity are indicated by *solid underlines*. *B*, Kyte-Doolittle hydropathy plot of Rhp2 is shown. The plot was constructed using the GENETYX-MAC program. *C*, shown is s secondary structure model of Rhp2 with putative 12 transmembrane (*TM*) spans. The region used as antigen is indicated by the *bold line*. The potential *N*-glycosylation and protein kinase C (*PKC*) phosphorylation sites are also shown.

CD728577), but we could not find the corresponding gene sequence in the genomic data base. Because the sequence length of the partial cDNA was not enough to align with other proteins, the chicken Rhp2 was excluded from the phylogenetic analysis.

Fig. 3 summarizes the exon/intron organizations of the Rh glycoprotein genes so far determined or deduced by comparing expressed sequence tag and genomic DNA databases, and reveals three patterns of organization. The *Rhag*, *Rhbg*, and *Rh30* genes consist of 10 exons, and the *Rhcg* genes have an additional noncoding exon (28). Interestingly, the *Rhp1* genes that are considered to be the most ancestral members of the family in eukaryote consist of 6–11 exons. In contrast, the *Rhp2* genes consist of only one single exon in the genomes of puffer fish and frog (1). To determine whether the *tsRhp2* gene also lacks the intron, we performed genomic PCR with primers positioned in the 5′- and 3′-UTR of the cDNA sequence. By touchdown PCR, a DNA fragment of ~1.6 kb was amplified (Fig. 3*A*). Direct sequence analysis revealed that the PCR product contained the full-length coding region and had no intron. This result indicated that the shark *Rhp2* gene consists of only one coding exon (Fig. 3*B*). To compare more extensively the exon/intron organizations of the Rh family genes, we performed a data base search of several vertebrates and invertebrates (Fig. 3*C*). *N. europaea*, which is assumed to be the earliest species with an Rh protein, has an *Rh* gene with no intron. As previously described, the human *RHAG*, *RH30*, *RHBG*, and *RHCG* genes consist of 10 coding exons (28), and similar exon/intron structures are observed in the orthologs of puffer fish. In contrast, the *Rhp2* genes of most species are intronless (Fig. 3*C*). Although, as mentioned above, the stop codon of the platypus *Rhp2* gene is not assignable because of the incomplete genome sequence, the gene seems to be intronless because the known sequence covers ~90% of the coding region. The exception is the zebrafish *Rhp2* gene that has an intron in its coding sequence (1).

Shark Rhp2 mRNA Is Exclusively Expressed in Renal Tubules of the Sinus Zone—In a previously study we found that two *Rhp2* genes are present in the genome of a teleost fish, *T. rubripes*. However, their mRNAs were not detected in any tissues tested including the gill, intestine, liver, spleen, and kidney (12). To determine the tissue distribution of Rhp2 mRNA of shark, Northern blot analysis was performed using total RNA preparations from 11 different tissues. A single transcript of ~2 kb was detected virtually exclusively in the kidney (Fig. 4).

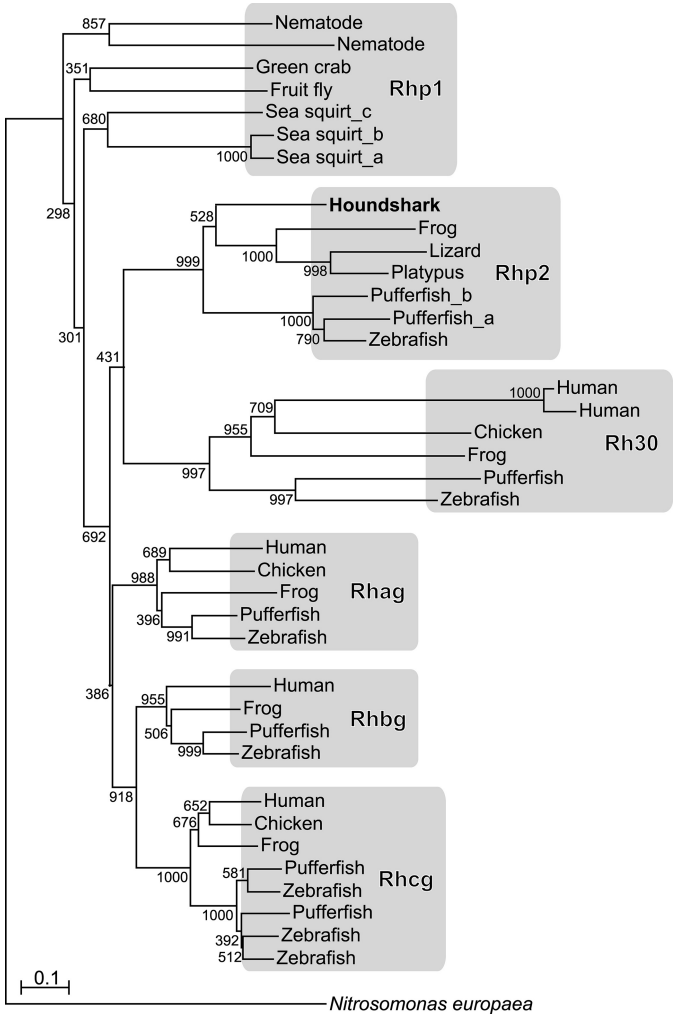

FIGURE 2. **Phylogenetic analysis of shark Rhp2 and other Rh family members.** The tree was constructed by the neighbor-join method with ClustalW program. The *scale bar* represents a genetic distance of 0.1 amino acid substitutions per site. The amino acid sequences used are as follows: Japanese banded hound shark *T. scyllium* Rhp2 (accession no. AB287007), human *H. sapiens* RhAG (AF237382), RhBG (NM_020407), RhCG (NM_016321), RhD (AJ299021), and RhCE (M34015), puffer fish *T. rubripes* Rhag (AB218979), Rhbg (AB218980), Rhcg1 (AB218981), Rhcg2 (AB218982), Rh30 (AAM48580), Rhp2a (AAM48575), and Rhp2b (AAM48576), zebrafish *D. rerio* Rhag (NP_998010), Rhbg (AAQ09527), Rhcg1 (AB286865), Rhcg2 (AB286866), Rhcg3 (AB286867), Rh30 (NP_001019990), and Rhp2 (NM_131547), platypus *O. anatinus* Rhp2 (XP_001507563, only a partial sequence available (residues 1–454) was used), western clawed frog *X. tropicalis* Rhag (AY865610), Rhbg (AY455819), Rhcg (AY271818), Rh30 (AY865609), and Rhp2 (AY865611), chicken *G. gallus* Rhag (AF531095), Rhcg (AY227357), and Rh30 (AY129071), nematode *C. elegans* Rhp1a (AAF97864) and Rhp1b (AAF97865), fruit fly *D. melanogaster* Rhp1 (NP_647940), sea squirt *C. intestinalis* Rhp1a (AY198126), Rhp1b (AY198127), and Rhp1c (AY198128), and nitrite-oxidizing bacteria *N. europaea* Rh (NP_840535).

We next performed *in situ* hybridization to determine the cellular location of Rhp2 mRNA in the shark kidney. The elasmobranch kidney is divided into two regions, the bundle and sinus zones. In the bundle zone, five tubular segments are tightly packed in parallel within a peritubular sheath to form a countercurrent system, whereas in the sinus zone, renal tubules meander convolutedly in large blood sinuses. Renal corpuscles are situated between the two zones (29). The renal tubule of the elasmobranch fishes consists of four loops, and the second and fourth loops are situated in the sinus zone (Fig. 5*F*). *In situ* hybridization revealed that Rhp2 mRNA is expressed in both (the second and fourth loops) of the tubule cells in the sinus zone (Fig. 5*A*), and no signal was detected in the bundle zone (Fig. 5, *A* and *C*) or in the renal corpuscles (Fig. 5*D*). No signal was observed in the negative control with a sense probe (Fig. 5*B*). Rhp2-negative tubules, which have obviously narrow diameters compared with the Rhp2-positive tubules, were also observed in the sinus zone (Fig. 5*E*). The distal portion of the second loop is known to consist of a thin layer of squamous cells and to have a relatively small diameter (29). This property of the second loop leads us to conclude that the Rhp2-negative tubules (Fig. 5*E*, *arrowheads*) correspond to the distal portion of the second loop (Fig. 5*F*).

Shark Rhp2 Is Localized on Basolateral Membranes of Renal Tubules in the Sinus Zone—For further analysis, we prepared an antiserum against tsRhp2 by immunizing rabbits with recombinant polypeptide corresponding to the C terminus of the protein, a region relatively variable among the Rh family members. The antiserum specificity was verified by Western blotting of lysates of HEK293T cells that transiently expressed tsRhp2. The antiserum detected a band of ~50 kDa in the lane of Rhp2-transfected cells but not in mock-transfected cells (Fig. 6*A*). Peptide *N*-glycosidase F treatment reduced the apparent molecular mass of Rhp2 to ~40 kDa, indicating that Rhp2 is *N*-glycosylated like other Rh glycoproteins. The apparent size of the band is slightly smaller than the calculated molecular mass of Rhp2, 52 kDa; this may be due to the highly hydrophobic nature of the protein. Similarly, slightly aberrant behaviors on SDS-PAGE were observed in other members of the Rh glycoprotein family (30–32). As expected, preincubation of the antiserum with the antigen peptide prevented immunostaining of both glycosylated and deglycosylated forms of Rhp2 (Fig. 6*A*). Among the known family members besides Rhp2 orthologs, Rh glycoproteins of puffer fish have the highest homology with the antigen region of Rhp2 (amino acids identities: fRhag, 38%; fRhbg, 43%; fRhcg1, 33%; fRhcg2, 32%). To assess the specificity of the antiserum, we conducted Western blotting with lysates of HEK293T cells that transiently expressed puffer fish Rh glycoproteins or hound shark Rhp2 with an N-terminal FLAG tag. The antiserum recognized FLAG-tagged Rhp2, and no cross-reactivity was observed with the puffer fish homologs. Immunoblotting with anti-FLAG verified expression and protein loading (supplemental Fig. 1).

Glycosylated and deglycosylated Rhp2 were also observed by immunoblotting of crude membrane fractions from shark kidney, indicating that Rhp2 is highly glycosylated in the native tissues (Fig. 6*A*). No band was observed in the liver, consistent with no expression of mRNA in the Northern blot (Fig. 4). These results indicate that the antiserum specifically recognizes the shark Rhp2 protein.

To determine the subcellular localization of Rhp2, we conducted immunohistochemistry. Clear labeling was observed in the basolateral membranes of renal tubule cells in the sinus zone but not in the bundle zone, consistent with the *in situ* hybridization results (Fig. 6*B*). No signal was observed in negative controls stained with preimmune serum and antiserum preincubated with immunizing antigen (Fig. 6*B*, *right panel*). It is known that the tubule cells of the proximal segment in the

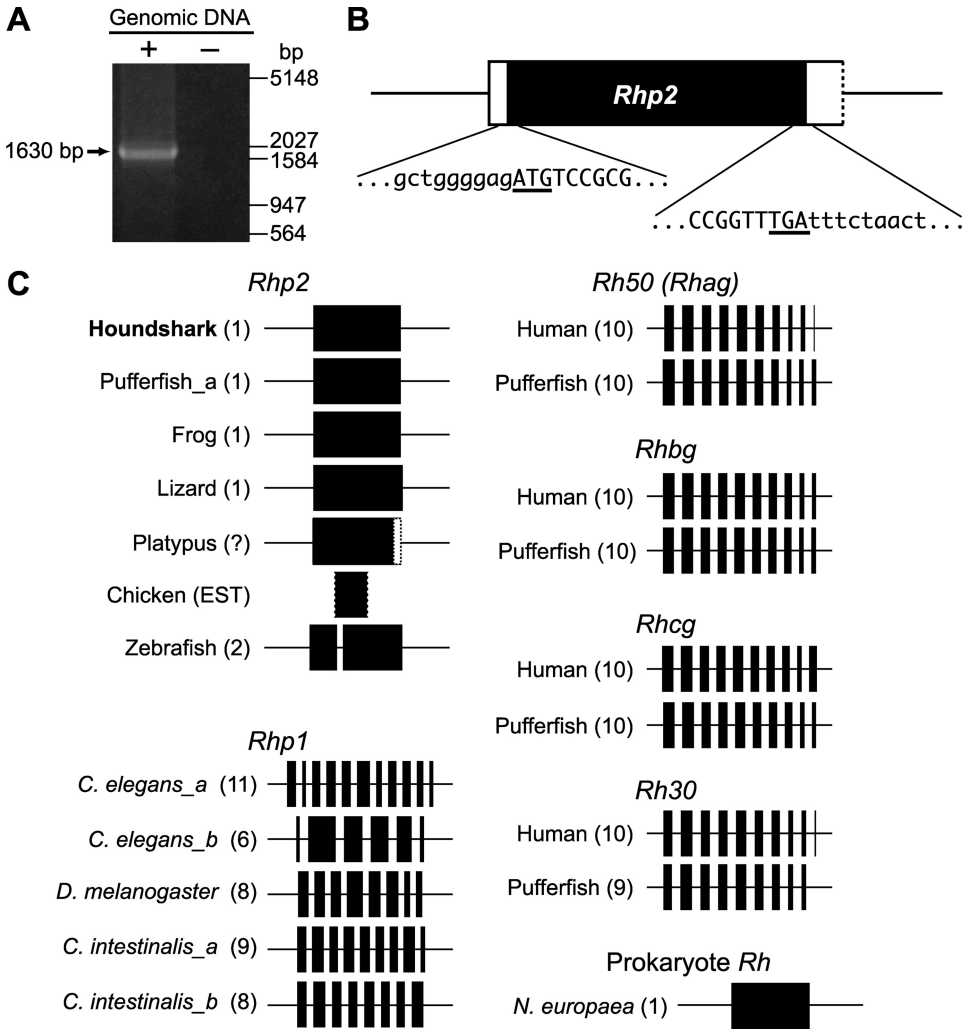

FIGURE 3. **Gene structures of shark *Rhp2* and other Rh family genes.** *A*, PCR product amplified from shark genome with Rhp2-specific primers is shown. Touchdown PCR was performed with shark genomic DNA and a primer set that positioned in 5′- and 3′-UTR of *Rhp2*. PCR product was separated by agarose gel electrophoresis and stained with ethidium bromide. *Numbers on the right* indicate the sizes of molecular weight markers. *B*, shown is a schematic representation of the shark *Rhp2* gene. *Filled* and *open boxes* indicate the coding and non-coding regions, respectively. Nucleotide sequences of the boundary of the coding and non-coding regions are shown, and start and stop codons are *underlined*. *C*, shown is a schematic representation of exon/intron structures of *Rh* family genes. *Filled boxes* indicate the coding exons, and the length of each reflects the number of amino acid residues, but introns are arbitrary length. The number of coding exons of each gene is indicated in the *parentheses*. A partial sequence of chicken Rhp2 (accession no. CD728577) found in the expressed sequence tag data base is also aligned.

second loop are rich in brush border microvilli, but the cells in other segments have no brush border (29). To distinguish the tubule segments by the presence of brush border, the actin-rich fibers in apical microvilli were stained with Alexa Fluor 488-conjugated phalloidin. Double staining with anti-Rhp2 and fluorescent phalloidin showed that Rhp2 is located in the basolateral membranes of the phalloidin-positive tubule cells (Fig. 6*C*), namely the proximal segment of the second loop. This conclusion was further confirmed by double staining for Rhp2 and Na^+/K^+-ATPase, which has been demonstrated to be highly expressed in the distal portion of second loop but weakly expressed in the proximal segment (21). As expected, cells that were strongly stained with anti-Na^+/K^+-ATPase were negative for Rhp2 (Fig. 6*D*). These results clearly demonstrate that Rhp2 is basolaterally localized in the epithelial cells of the proximal segment of the second loop of the renal tubule. Immunostaining of serial sections using anti-Rhp2 and anti-V-ATPase antisera showed that V-ATPase was localized in the apical membrane of Rhp2-positive tubules (Fig. 6*E*).

Expression of Rhp2 Is Regulated by Environmental Salinity—To maintain the body fluid osmolality, hepatic urea synthesis and renal urea reabsoption rates of elasmobranch fishes are regulated by environmental salinity (For review, see Refs. 33 and 34). We previously described that plasma urea levels of the hound sharks used here were up-regulated in the concentrated seawater compared with diluted seawater (22). To elucidate whether Rhp2 is involved in osmoregulation for adapting to varying environmental salinity, we performed quantitative real-time PCR on kidneys from sharks that were acclimated to 100% (control), 60% (low), or 130% (high) seawater. Expression of Rhp2 mRNA in the high salinity group was significantly increased compared with the low salinity group (Fig. 7*A*). We further performed Western blotting to confirm that the protein level of Rhp2 is also changed by different salinity environments. In addition to the above experiment, sharks were acclimated to lower salinity (30%). The levels of Rhp2 protein were slightly reduced in 60% salinity and further decreased in 30% seawater (Fig. 7*B*). Meanwhile, acclimation to 130% seawater induced increments of Rhp2 protein levels in a time-dependent manner (Fig. 7*B*). These data indicated that Rhp2 expression was regulated by environmental salinity.

Functional Analysis of Shark Rhp2—To date, no studies have been done to functionally characterize Rhp2 from any species. Because the amino acid sequence of the shark Rhp2 is very similar to other Rh glycoproteins capable of transporting ammonia, we tested the ability of tsRhp2 to transport MA, an analog of ammonia, by expression in *Xenopus* oocytes. [^{14}C]MA flux uptake, mediated by expression of tsRhp2, was 4–5-fold greater compared with uptake in the water-injected control oocytes at 1.5 mM substrate concentration (Fig. 8*A*). Because elasmobranch fish reabsorb urea to maintain tissue osmolarity in seawater and also adsorb TMAO to counterbalance urea, we tested the possibility that these might be alternative substrates for Rhp2 by competitive inhibition experiments. MA uptake was competitively inhibited in the presence of

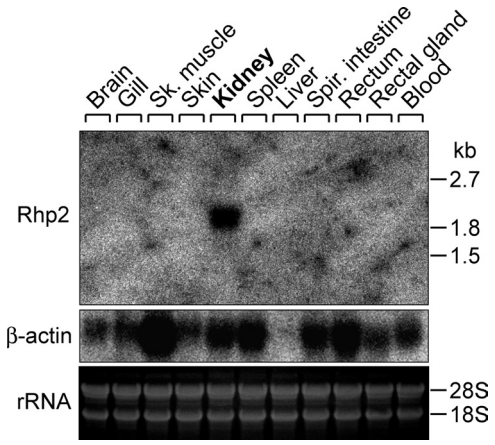

FIGURE 4. **Kidney-specific expression of shark *Rhp2* gene transcript.** Northern blot analysis was performed using 10 μg of total RNA from each tissue. β-Actin was used as an internal control. The 28 S and 18 S rRNA bands visualized by ethidium bromide staining are also shown to demonstrate equal loading and the quality of RNA preparations. *Numbers on the right* indicate the sizes of molecular weight markers. *Sk*, skeletal; *Spir*, spiral.

ammonium chloride but was not competed with TMAO or by urea (Fig. 8*B*). Uptake was also not inhibited by the addition of tetramethylammonium chloride or tetraethylammonium chloride (data not shown). These results are compatible with ammonia as the actual substrate for Rhp2.

To further characterize transport, the effect of modulating the membrane potential was examined by replacement of Na^+ in the uptake buffer (100 mM NaCl) with high K^+ (100 mM KCl). The oocytes depolarize, but uptake was unaffected (Fig. 8*C*), indicating that transport by tsRhp2 is not a conductive process. To ascertain if transport was responsive to the protonated or unprotonated species, uptake was measured in buffers that contained equivalent concentrations of unprotonated MA (7.6 μM) but that had a 10-fold difference in the concentration of protonated MA^+ (Fig. 8*D*). The uptake rate differed significantly in the presence of a fixed concentration of the unprotonated substrate, with the uptake rate proportional to the concentration of protonated MA^+. To determine the kinetics of transport, the rate of uptake was measured with increasing concentrations of substrate (Fig. 8*E*). The data were well fitted with a Michaelis-Menten equation with an EC_{50} (K_m) for tsRhp2 of 1.5 mM.

DISCUSSION

In this study we isolated and characterized a novel member of the Rh glycoprotein family from the shark kidney. This protein, named tsRhp2, is predicted to have 12 transmembrane spans and an *N*-glycosylation site in the first extracellular loop, features well conserved in vertebrate Rh glycoproteins (Fig. 1). Subsequent data base mining and a phylogenetic study revealed that the *Rhp2* gene is widely distributed among vertebrates including platypus, a semiaquatic monotreme (a most distant mammalian relative), but not in the genomes of the human, mouse, and rat (Fig. 2). Huang *et al.* (1) postulate that *Rhp2* is probably the most ancient gene among the Rh family because it lacks introns and is most closely related to *N. europaea Rh* and invertebrate *Rhp1*. Our comparison of the cDNA and the corresponding genomic DNA sequences showed that the shark

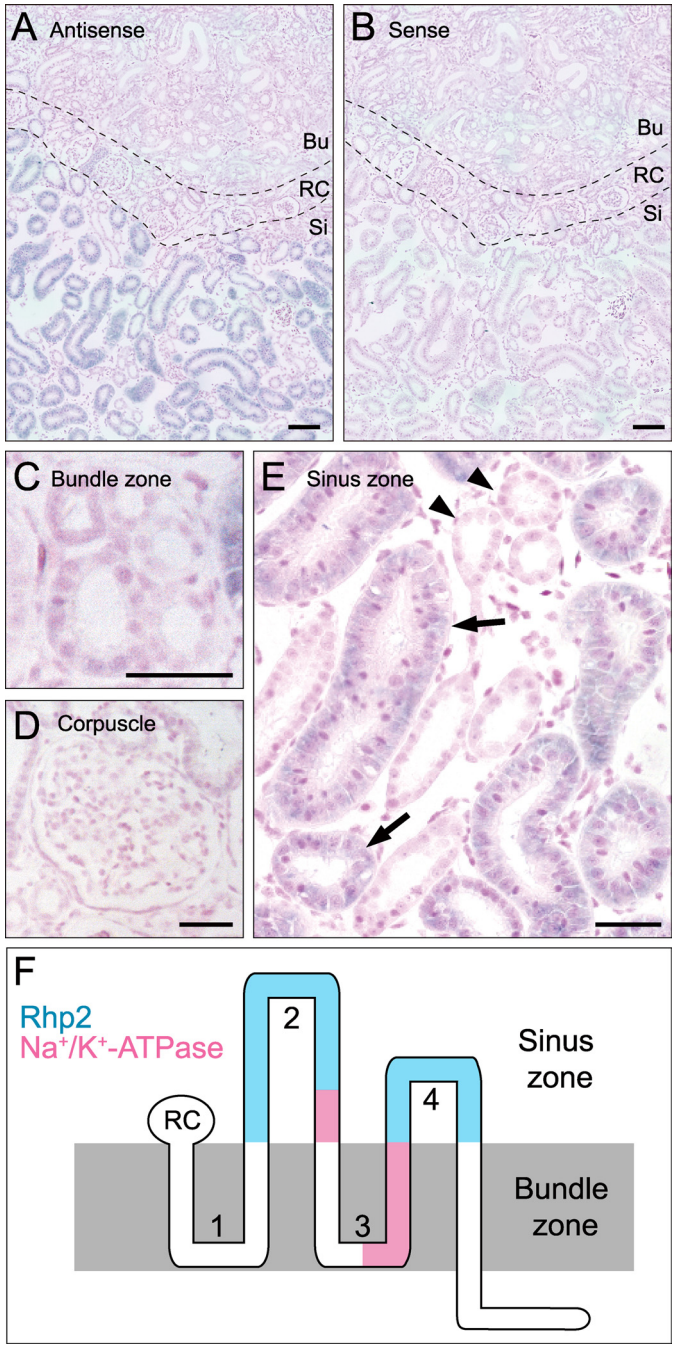

FIGURE 5. **Localization of Rhp2 mRNA in the renal tubule cells of sinus zone.** *A* and *B*, *in situ* hybridization of Rhp2 mRNA in the shark kidney using DIG-labeled antisense (*A*) and sense (*B*) probes is shown. The probes were detected with alkaline phosphatase-conjugated anti-DIG antibody and nitro blue tetrazolium/5-bromo-4-chloro-3-indolyl phosphate substrates (*blue*). Kernechtrot was used for counterstaining of the nucleus (*pink*). *Bu*, bundle zone; *RC*, renal corpuscle-rich region; *Si*, sinus zone. *Bars*, 100 μm. *C* and *D*, shown is a magnified view of five tubular segments in the bundle zone (*C*) and renal corpuscle (*D*). *E*, shown is a magnified view of Rhp2-positive and -negative tubules in the sinus zone. Rhp2-positive tubules (*arrows*) have a comparatively larger diameter than those of the Rhp2-negative tubules (*arrowheads*). *Bars*, 50 μm. *F*, shown is a schematic diagram of the single nephron. Blue-colored segments indicate expressions of Rhp2 mRNA. The regions rich in Na^+/K^+-ATPase (*pink*) were identified by the previous studies of Hyodo *et al.* (21). *RC*, renal corpuscle.

Rhp2 gene also lacks introns. In contrast, the *Rhp1* gene, which is previously assumed to be the most ancestral *Rh* cluster in eukaryotes, has five or more introns in all species examined.

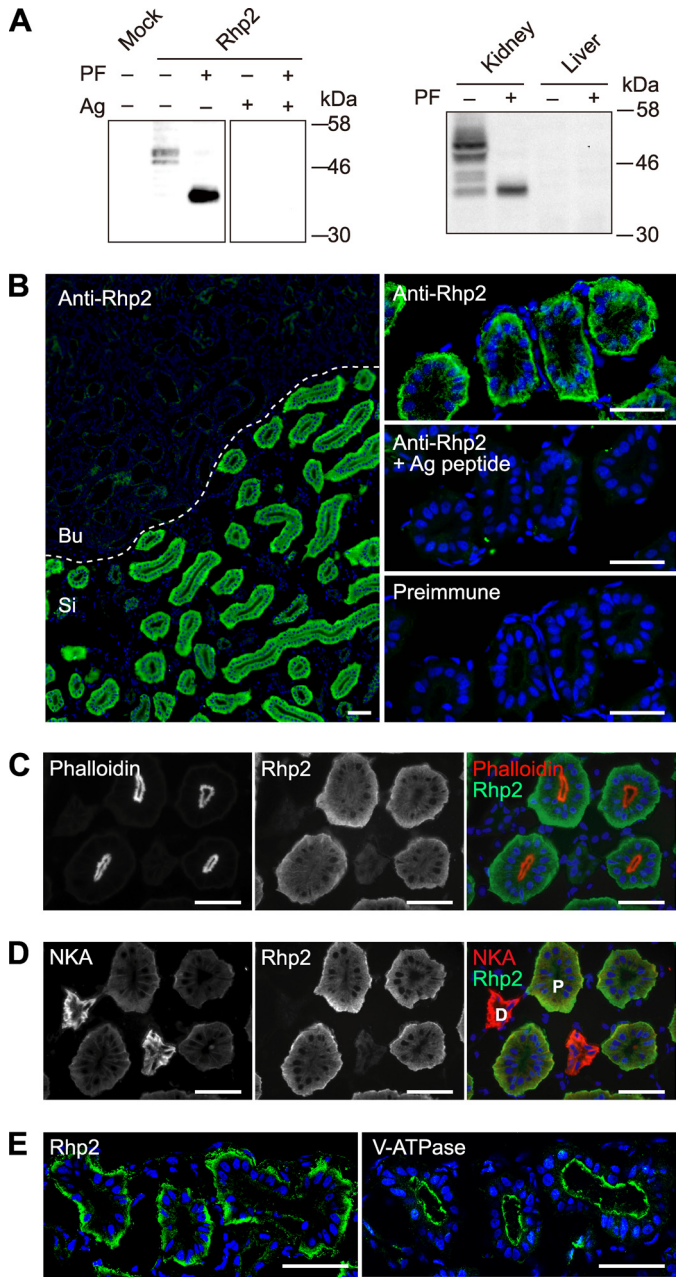

FIGURE 6. **Basolateral localization of Rhp2 in the renal tubule cells.** *A*, Western blotting of Rhp2 is shown. HEK293T cells were transiently transfected with pcDNA3.1 (*Mock*) or pcDNA-Rhp2, and the crude membrane fractions were subjected to 10% SDS-PAGE and immunoblotting (*left panel*). The crude membrane fractions from shark kidney and liver were subjected to 10% SDS-PAGE and immunoblotting (*right panel*). Plus (+) symbols indicate treatment of samples with peptide *N*-glycosidase F (*PF*) or preabsorption of antiserum with the antigen (*Ag*) peptide. *B*, immunohistochemistry of shark kidney using anti-Rhp2 antiserum is shown. Bound antibodies were detected with Alexa Fluor 488-labeled secondary antibody (*green*), and the nucleus was stained with Hoechst 33342 (*blue*). Rhp2-positive tubules were localized in the sinus zone. *Bu*, bundle zone; *Si*, sinus zone (*left panel*). Serial sections were stained with anti-Rhp2 antiserum preincubated with or without excess antigen or preimmune serum (*right panels*). *C*, double staining with anti-Rhp2 and TRITC-labeled phalloidin is shown. The anti-Rhp2 antiserum (*green*) and phalloidin (*red*) stained basolateral and apical membranes, respectively, of the same tubule cells. *D*, shown is double staining of Rhp2 and Na^+/K^+-ATPase (*NKA*). Rhp2-negative tubules were strongly stained with anti-Na^+/K^+-ATPase (*red*), whereas Rhp2-positive tubules (*green*) were weekly stained with anti-Na^+/K^+-ATPase. *P*, proximal; *D*, distal. *E*, serial sections were stained with anti-Rhp2 or anti-V-ATPase antisera. Bound antibodies were detected with Alexa Fluor 488-labeled secondary antibody (*green*), and the nucleus was stained with Hoechst 33342 (*blue*). *Bars*, 50 μm.

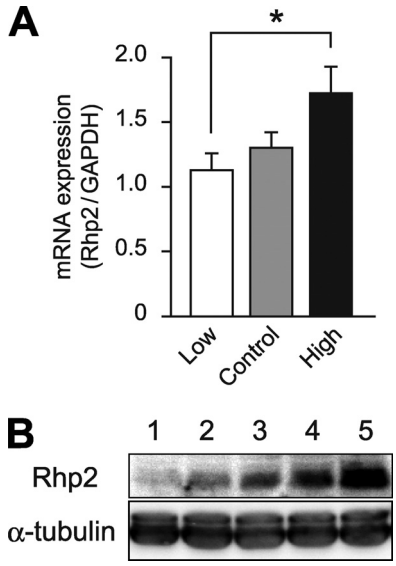

FIGURE 7. **Changes in Rhp2 mRNA and protein levels dependent on the environmental salinity.** *A*, sharks were acclimated to 100% (*Control*), 60% (*Low*), or 130% seawater (*High*) for 2 days, and expressions of Rhp2 mRNA in kidney were determined by real-time PCR. The abundance of Rhp2 mRNA is expressed as a ratio to glyceraldehyde-3-phosphate dehydrogenase (*GAPDH*) mRNA levels. The *asterisk* indicates $p < 0.05$ by the Tukey-Kramer test. Values are the means ± S.E. ($n = 6–8$). *B*, sharks were acclimated to the following conditions: 7 days in 30% seawater (*lane 1*), 2 days in 60% seawater (*lane 2*) and 100% seawater (*lane 3*), 2 days in 130% seawater (*lane 4*), and 7 days in 130% seawater (*lane 5*). Kidney lysates were extracted individually, and equal amounts of proteins were pooled in each group ($n = 4–10$). All samples were treated with peptide *N*-glycosidase F and subjected to 10% SDS-PAGE and immunoblotting. α-Tubulin was used as an internal control.

From these data, two hypotheses have emerged to explain the origin of the *Rhp2* gene; 1) *Rhp2* diverged directly from the precursor intronless *Rh* gene such as that seen in *N. europaea*, or 2) *Rhp2* arose by retroposition of a processed mRNA of other *Rh* genes containing introns like invertebrate *Rhp1*. At present, both possibilities remain. Additionally, we have also isolated the partial cDNA fragments encoding Rhag, Rhbg, and Rhcg from hound shark tissues.[6] This fact indicates that a set of Rh glycoproteins (Rhag, Rhbg, Rhcg, and Rhp2), which are seen in higher vertebrates, were already present before divergence of elasmobranch and teleost fishes. To understand the origin of Rhp2, it will be informative to know whether *Rhp2* and other *Rh*-related genes exist on the genomes of lamprey and/or hagfish, which are more primitive than shark.

Oocyte expression studies showed that tsRhp2 facilitates MA transport, an analog of ammonia. The K_m value (1.5 mM, Fig. 8*E*) was similar to that reported for human RhAG (8), and tsRhp2 also had a higher affinity for substrate than human RhBG and RhCG (K_m 2.5 and 10 mM, respectively) (5). Like other Rh glycoproteins, the rate of transport by Rhp2 responded to changes in the concentration of NH_4^+ species when the NH_3 concentration was held constant (Fig. 8*D*), but uptake was independent of the membrane potential (Fig. 8*C*). These data suggest that transport is responsive to NH_4^+ concentration, with net transport of the neutral species. However, the exact mechanism of transport (NH_4^+/H^+ exchange or by loss of H^+

[6] T. Nakada, and S. Hirose, unpublished data.

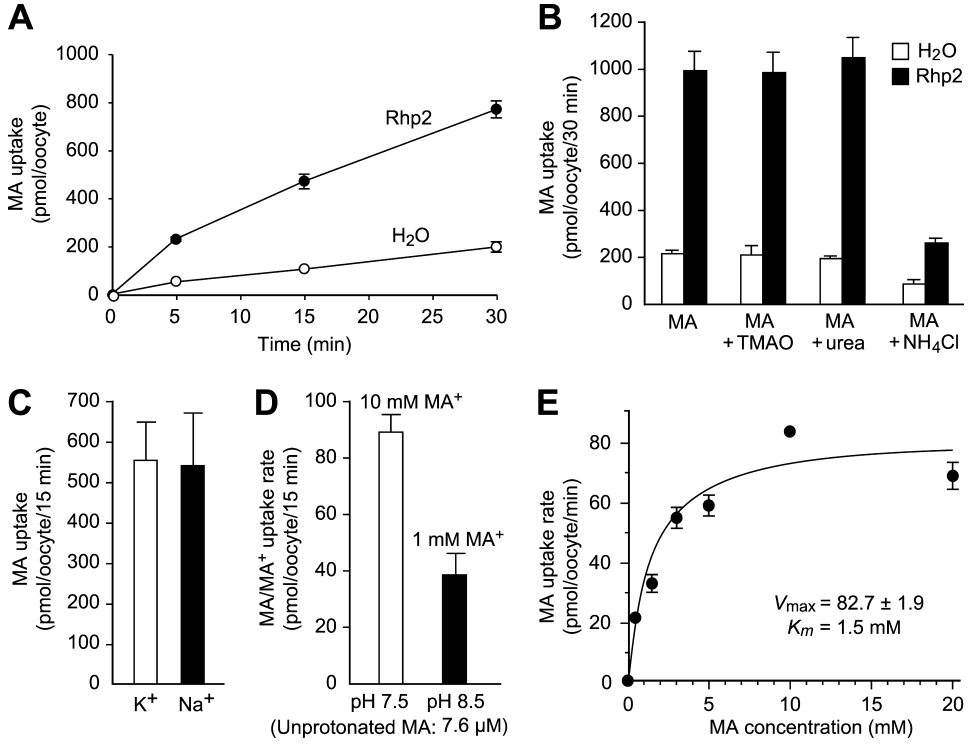

FIGURE 8. **Functional characterization of Rhp2 expressed in *Xenopus* oocytes.** *A*, shark Rhp2 cRNA-injected oocytes were compared with water-injected controls. Groups of six oocytes were analyzed at each time point in uptake buffer with [^{14}C]methylammonium with 1.5 mM MA at pH 7.5 and reported as pmol/oocyte. *B*, inhibition of Rhp2-mediated MA uptake is shown. Groups of four oocytes were analyzed in uptake buffer as above in the presence of 10 mM TMAO, 10 mM urea, or 10 mM NH_4Cl. Data in *A* and *B* are representative of three independent experiments. *C*, the effect of oocyte membrane depolarization on MA uptake is shown. Uptake in standard Na^+ buffer as above and in K^+ buffer in which NaCl was replaced by KCl is shown. Values are the means ± S.E. ($n = 3$) for groups of six oocytes. *D*, MA/MA^+ uptake rates in the presence of a fixed concentration of 7.6 μM unprotonated species is shown. Equivalent concentration of unprotonated substrate was generated with a 10-fold difference in total (protonated and unprotonated) MA concentration (indicated *above the bars*) at the specific pH values shown. Values are the means ± S.E. ($n = 3$) of groups of six oocytes, and uptake values for water-injected controls have been subtracted. *E*, shown are transport kinetics. Rate of uptake was a saturable function of total MA/MA^+. The curve represents the Michaelis-Menten fit, and values are the means ± S.E. ($n = 3$–6) for groups of six oocytes. Water-injected s controls have been subtracted.

from NH_4^+ with transport of NH_3) is not possible to resolve from the present study.

Unlike most marine teleost fishes, the marine elasmobranch, which include sharks and rays, have evolved the technique of reabsorbing and retaining urea (0.2–0.5 M) in their plasma and tissues to maintain body osmolarities nearly equal to that of seawater (34–37). To counteract the destabilizing effects of the urea on proteins, the elasmobranch fishes employ TMAO (40–80 mM). Because TMAO should also be reabsorbed in the kidney, we tested the hypothesis that Rhp2 may be the TMAO transporter involved in its renal reabsorption, but this turned out not to be the case by functional characterization.

In the previous study on seawater puffer fish, *T. rubripes*, we isolated two cDNA fragments homologous to Rhp2. However, Northern blot analysis found no expression in any tissues tested including the gill, liver, and kidney (12). In contrast, we found that shark Rhp2 is highly and exclusively expressed in the kidney. In mammals, renal ammonia genesis occurs in the proximal tubule cells by degradation of glutamate, which is taken up from plasma across the basolateral membrane to contribute to the H^+ excretion. The produced ammonia is secreted into the luminal tract and is reabsorbed at the thick ascending limb to accumulate in the medullary interstitium. The ammonia gradient between the medullary interstitium and the lumen of the collecting duct allows ammonia to translocate into the luminal tract again. RhBG and RhCG are expressed in the same tubular cells of the collecting duct and may be involved in the final step of the transport processes (5, 32, 38–40).

In contrast to the well characterized mammalian renal ammonia transport systems, there are few studies on those of elasmobranch fish. *In situ* hybridization and immunohistochemistry showed that Rhp2 was basolaterally localized in the renal tubule cells of the second and fourth loops in the sinus zone. Although several ion transporters have been localized to a specific segment of renal tubules in elasmobranch fish (21, 41–45), the functional significance of ammonia transport in the second and fourth loops is poorly understood. From its cellular and subcellular location, we assumed that Rhp2 facilitates ammonia transport across the basolateral membranes of renal tubule cells, but concerning the direction of the transport, we cannot conclude whether it mediates ammonia reabsorption or secretion *in vivo*. The up-regulation of renal ammonia secretion was observed in elasmobranch fish under an acid load (46, 47). This fact suggests an enhanced diffusion of ammonia from sinus blood into urine. However, compared with the relatively large role of the fish gill in ammonia elimination and acid-base regulation, the renal ammonia excretion rate is very low. Furthermore, King and Goldstein (46) suggested that this renal ammonia excretion under acid load may occur by the degradation of glutamate, which does not depend on basolateral ammonia transport. Because Rhp2 is localized in basolateral membranes of epithelial cells, it is likely not involved in ammonia excretion in acidosis. Compared with the relatively high urine/plasma ammonia ratio in mammals (>500), the ratio is only ~3 in elasmobranch fish (47). Because 60–80% of the filtered water is reabsorbed in the resting elasmobranch kidney (48), ammonia in the primary urine seems to be concentrated about 2.5–4-fold relative to plasma even without diffusion and/or carrier-mediated transport systems. These facts suggest that active ammonia secretion is absent or very low in the elasmobranch kidney under resting conditions.

Alternatively, the basolateral Rhp2 may contribute to the ammonia reabsorption from the filtered urine. The pH difference between urine (~5.8) and plasma (~7.9) leads to a steep gradient of NH_3 (unprotonated state). In these pH conditions

the concentration of plasma NH_3 is calculated to be ~40-fold higher than its urinary concentration even though total ammonia ($NH_4^+ + NH_3$) concentration is 3-fold higher in urine. This NH_3 gradient likely drives its passive diffusion from blood toward the luminal tract, resulting in urinary loss of a large amount of ammonia. Nevertheless, the urine/plasma ammonia ratio is considerably low compared with that in mammals (47), suggesting that ammonia is actively reabsorbed in the elasmobranch nephron to prevent excessive loss. This is reasonable because ammonia is one of the most important sources for synthesizing urea, which is required to maintain the body fluid osmolality of elasmobranch fish. Quantitative PCR analysis and Western blotting showed that renal expression of Rhp2 was increased in concentrated seawater compared with that in diluted seawater (Fig. 7), suggesting that Rhp2 is involved in adapting to environmental salinity challenge. It is known that plasma urea concentration is increased when elasmobranch fishes are acclimated to high salinity environment. Indeed, we previously reported that plasma urea concentration of shark acclimated to 130% seawater was ~1.7-fold higher than that under 60% seawater condition (22). These results provide strong support for the hypothesis that Rhp2 is involved in ammonia reabsorption as a source for urea synthesis. In this model, an active NH_4^+ uptake system is necessary at the apical membrane of Rhp2-expressing cells. Various ion pumps or transporters such as Na^+/K^+-ATPase, Na^+-K^+-$2Cl^-$ cotransporter (NKCC), K^+-Cl^- cotransporter, and H^+/K^+-ATPase are known to accept NH_4^+ as substrate in place of K^+ (for review, see Ref. 49). Among these molecules, NKCC2 is located at the apical membranes of tubular cells in the thick ascending limb of mammalian kidneys and takes up the majority of NH_4^+ from the luminal tract (50). In the elasmobranch kidney, NKCC immunoreactivity was detected in the apical membranes of the distal tubule and of a portion of proximal tubule in the sinus zone (43). It may transport NH_4^+ into the cell from the luminal tract in a similar fashion as in mammalian kidneys (Fig. 9). The oocyte study suggested that the Rhp2-mediated transport is responsive to NH_4^+ concentration, with net transport of the neutral species (Fig. 8). These data also suggest that net NH_3 transport by basolateral Rhp2 results in H^+ accumulation in the tubular epithelial cells. Apical localization of V-ATPase in the same tubule cells is ideal for secretion of the remaining H^+ into luminal space (Fig. 6*E*). A major portion of ammonia, reabsorbed by the cooperative action of apical NKCC, V-ATPase, and basolateral Rhp2, should be used for the hepatic or extrahepatic ornithine-urea cycle.

Another possible role of tsRhp2 is that this protein might act as a CO_2 channel. It has been suggested that the Rh glycoprotein might accept CO_2 as its substrate (51–56). The proximal tubule, where Rhp2 is expressed, is the major site for HCO_3^- reabsorption for elasmobranch fish (57, 58). Because urine of seawater fishes contains large quantities of Mg^{2+}, it will form precipitates as $Mg(OH)_2$ or $MgHPO_4$ if the urinary pH exceeds 6.0. To prevent this, elasmobranch fish reabsorb HCO_3^- and maintain the urine at an acid pH (5.7–5.8). Interestingly, renal HCO_3^- reabsorption in seawater fish is a carbonic anhydrase-independent process, unlike other animals such as freshwater fish and mammals (57, 58). If Rhp2 facilitates diffusion of CO_2 gas across the basolateral membrane of the renal tubule cells, it would be beneficial for the carbonic anhydrase-independent system to work efficiently. Although recent studies reveal that mammalian RhAG has significantly greater selectivity for NH_3 compared with CO_2 (59), further studies are necessary to clarify a possible role if any of Rhp2 in renal CO_2/HCO_3^- reabsorption.

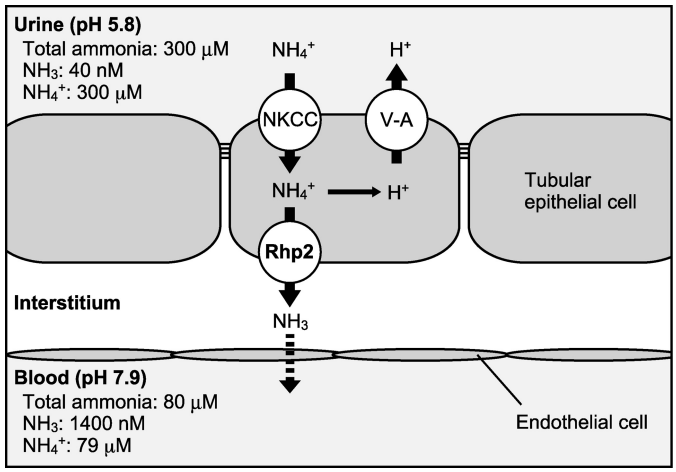

FIGURE 9. **A predicted model of ammonia reabsorption mediated by shark Rhp2.** To prevent excessive loss of ammonia, Rhp2, NKCC-like transporter, and vacuolar-type H^+-ATPase act cooperatively to reabsorb the ammonia. Apical NKCC-like transporter incorporates NH_4^+ (in place of K^+) from lumen into the tubular epithelial cells. Accumulation of intracellular ammonia allows basolateral Rhp2 to transport the ammonia toward interstitium and blood sinus side. The remaining H^+ is secreted into the luminal tract by V-ATPase. Values of ammonia and pH are referred to those of spiny dogfish shark (*Squalus acanthias*) taken from Wood *et al.* (47). *V-A*, vacuolar-type H^+-ATPase.

Acknowledgments—We thank Masafumi Ohara for technical assistance, Dr. Masaki Kajikawa for useful discussions, Yoichi Noguchi and Kazuo Okubo of Genostaff for technical assistance in in situ hybridization histochemistry, and Setsuko Sato for secretarial assistance.

REFERENCES

1. Huang, C. H., and Peng, J. (2005) *Proc. Natl. Acad. Sci. U.S.A.* **102,** 15512–15517
2. Bakouh, N., Benjelloun, F., Hulin, P., Brouillard, F., Edelman, A., Chérif-Zahar, B., and Planelles, G. (2004) *J. Biol. Chem.* **279,** 15975–15983
3. Benjelloun, F., Bakouh, N., Fritsch, J., Hulin, P., Lipecka, J., Edelman, A., Planelles, G., Thomas, S. R., and Chérif-Zahar, B. (2005) *Pflugers Arch.* **450,** 155–167
4. Ludewig, U. (2004) *J. Physiol.* **559,** 751–759
5. Mak, D. O., Dang, B., Weiner, I. D., Foskett, J. K., and Westhoff, C. M. (2006) *Am. J. Physiol. Renal Physiol.* **290,** F297–F305
6. Marini, A. M., Matassi, G., Raynal, V., André, B., Cartron, J. P., and Chérif-Zahar, B. (2000) *Nat. Genet.* **26,** 341–344
7. Ripoche, P., Bertrand, O., Gane, P., Birkenmeier, C., Colin, Y., and Cartron, J. P. (2004) *Proc. Natl. Acad. Sci. U.S.A.* **101,** 17222–17227
8. Westhoff, C. M., Ferreri-Jacobia, M., Mak, D. O., and Foskett, J. K. (2002) *J. Biol. Chem.* **277,** 12499–12502
9. Westhoff, C. M., Siegel, D. L., Burd, C. G., and Foskett, J. K. (2004) *J. Biol. Chem.* **279,** 17443–17448
10. Weihrauch, D., Morris, S., and Towle, D. W. (2004) *J. Exp. Biol.* **207,** 4491–4504
11. Ji, Q., Hashmi, S., Liu, Z., Zhang, J., Chen, Y., and Huang, C. H. (2006) *Proc. Natl. Acad. Sci. U.S.A.* **103,** 5881–5886
12. Nakada, T., Westhoff, C. M., Kato, A., and Hirose, S. (2007) *FASEB J.* **21,** 1067–1074

13. Hung, C. C., Nawata, C. M., Wood, C. M., and Wright, P. A. (2008) *J. Exp. Zool. A Ecol. Genet. Physiol.* **309,** 262–268
14. Nawata, C. M., Hung, C. C., Tsui, T. K., Wilson, J. M., Wright, P. A., and Wood, C. M. (2007) *Physiol. Genomics* **31,** 463–474
15. Nawata, C. M., and Wood, C. M. (2008) *J. Exp. Biol.* **211,** 3226–3236
16. Tsui, T. K., Hung, C. Y., Nawata, C. M., Wilson, J. M., Wright, P. A., and Wood, C. M. (2009) *J. Exp. Biol.* **212,** 878–892
17. Hung, C. Y., Tsui, K. N., Wilson, J. M., Nawata, C. M., Wood, C. M., and Wright, P. A. (2007) *J. Exp. Biol.* **210,** 2419–2429
18. Braun, M. H., Steele, S. L., Ekker, M., and Perry, S. F. (2009) *Am. J. Physiol. Renal Physiol.* **296,** F994–F1005
19. Nakada, T., Hoshijima, K., Esaki, M., Nagayoshi, S., Kawakami, K., and Hirose, S. (2007) *Am. J. Physiol. Regul. Integr. Comp. Physiol.* **293,** R1743–R1753
20. Shih, T. H., Horng, J. L., Hwang, P. P., and Lin, L. Y. (2008) *Am. J. Physiol. Cell Physiol.* **295,** C1625–C1632
21. Hyodo, S., Katoh, F., Kaneko, T., and Takei, Y. (2004) *J. Exp. Biol.* **207,** 347–356
22. Hyodo, S., Tsukada, T., and Takei, Y. (2004) *Gen. Comp. Endocrinol.* **138,** 97–104
23. American Physiological Society (2002) *Am. J. Physiol. Regul. Integr. Comp. Physiol.* **283,** R281–R283
24. Nakada, T., Zandi-Nejad, K., Kurita, Y., Kudo, H., Broumand, V., Kwon, C. Y., Mercado, A., Mount, D. B., and Hirose, S. (2005) *Am. J. Physiol. Regul. Integr. Comp. Physiol.* **289,** R575–R585
25. Mistry, A. C., Honda, S., Hirata, T., Kato, A., and Hirose, S. (2001) *Am. J. Physiol. Regul. Integr. Comp. Physiol.* **281,** R1594–R1604
26. Hirata, T., Kaneko, T., Ono, T., Nakazato, T., Furukawa, N., Hasegawa, S., Wakabayashi, S., Shigekawa, M., Chang, M. H., Romero, M. F., and Hirose, S. (2003) *Am. J. Physiol. Regul. Integr. Comp. Physiol.* **284,** R1199–R1212
27. Yamaguchi, Y., Takaki, S., and Hyodo, S. (2009) *J. Exp. Zool. A Ecol. Genet. Physiol.* **311,** 705–718
28. Huang, C. H., and Liu, P. Z. (2001) *Blood Cells Mol. Dis.* **27,** 90–101
29. Lacy, E. R., and Reale, E. (1985) *Anat. Embryol.* **173,** 163–186
30. Liu, Z., Chen, Y., Mo, R., Hui, C., Cheng, J. F., Mohandas, N., and Huang, C. H. (2000) *J. Biol. Chem.* **275,** 25641–25651
31. Liu, Z., Peng, J., Mo, R., Hui, C., and Huang, C. H. (2001) *J. Biol. Chem.* **276,** 1424–1433
32. Quentin, F., Eladari, D., Cheval, L., Lopez, C., Goossens, D., Colin, Y., Cartron, J. P., Paillard, M., and Chambrey, R. (2003) *J. Am. Soc. Nephrol.* **14,** 545–554
33. Hazon, N., Wells, A., Pillans, R. D., Good, J. P., Gary Anderson, W., and Franklin, C. E. (2003) *Comp. Biochem. Physiol. B Biochem. Mol. Biol.* **136,** 685–700
34. McDonald, M. D., Smith, C. P., and Walsh, P. J. (2006) *J. Membr. Biol.* **212,** 93–107
35. Poulsen, J. M. (1981) *Sphyrna Tiburo. Comp. Biochem. Physiol* **70,** 127–131
36. Smith, H. W. (1931) *Am. J. Physiol.* **98,** 279–295
37. Thorson, T. B. (1962) *Science* **138,** 688–690
38. Biver, S., Belge, H., Bourgeois, S., Van Vooren, P., Nowik, M., Scohy, S., Houillier, P., Szpirer, J., Szpirer, C., Wagner, C. A., Devuyst, O., and Marini, A. M. (2008) *Nature* **456,** 339–343
39. Handlogten, M. E., Hong, S. P., Westhoff, C. M., and Weiner, I. D. (2004) *Am. J. Physiol. Renal Physiol.* **287,** F628–F638
40. Verlander, J. W., Miller, R. T., Frank, A. E., Royaux, I. E., Kim, Y. H., and Weiner, I. D. (2003) *Am. J. Physiol. Renal Physiol.* **284,** F323–F337
41. Althoff, T., Hentschel, H., Luig, J., Schütz, H., Kasch, M., and Kinne, R. K. (2006) *Am. J. Physiol. Regul. Integr. Comp. Physiol.* **290,** R1094–R1104
42. Althoff, T., Hentschel, H., Luig, J., Schütz, H., Kasch, M., and Kinne, R. K. (2007) *Am. J. Physiol. Regul. Integr. Comp. Physiol.* **292,** R2391–R2399
43. Biemesderfer, D., Payne, J. A., Lytle, C. Y., and Forbush, B., 3rd (1996) *Am. J. Physiol.* **270,** F927–F936
44. Cai, S. Y., Soroka, C. J., Ballatori, N., and Boyer, J. L. (2003) *Am. J. Physiol. Regul. Integr. Comp. Physiol.* **284,** R125–R130
45. Swenson, E. R., Fine, A. D., Maren, T. H., Reale, E., Lacy, E. R., and Smolka, A. J. (1994) *Am. J. Physiol.* **267,** F639–F645
46. King, P. A., and Goldstein, L. (1983) *Am. J. Physiol.* **245,** R581–R589
47. Wood, C., Pärt, P., and Wright, P. (1995) *J. Exp. Biol.* **198,** 1545–1558
48. Evans, D. H. (1993) in *The Physiology of Fishes* (Evans, D. H., ed) pp. 315–341, CRC Press, Boca Raton, FL
49. Attmane-Elakeb, A., Amlal, H., and Bichara, M. (2001) *Am. J. Physiol. Renal Physiol.* **280,** F1–F9
50. Good, D. W., Knepper, M. A., and Burg, M. B. (1984) *Am. J. Physiol.* **247,** F35–F44
51. Endeward, V., Cartron, J. P., Ripoche, P., and Gros, G. (2006) *Transfus. Clin. Biol.* **13,** 123–127
52. Endeward, V., Cartron, J. P., Ripoche, P., and Gros, G. (2008) *FASEB J.* **22,** 64–73
53. Kustu, S., and Inwood, W. (2006) *Transfus. Clin. Biol.* **13,** 103–110
54. Li, X., Jayachandran, S., Nguyen, H. H., and Chan, M. K. (2007) *Proc. Natl. Acad. Sci. U.S.A.* **104,** 19279–19284
55. Soupene, E., Inwood, W., and Kustu, S. (2004) *Proc. Natl. Acad. Sci. U.S.A.* **101,** 7787–7792
56. Soupene, E., King, N., Feild, E., Liu, P., Niyogi, K. K., Huang, C. H., and Kustu, S. (2002) *Proc. Natl. Acad. Sci. U.S.A.* **99,** 7769–7773
57. Deetjen, P., and Maren, T. (1974) *Pflugers Arch.* **346,** 25–30
58. Hodler, J., Heinemann, H. O., Fishman, A. P., and Smith, H. W. (1955) *Am. J. Physiol.* **183,** 155–162
59. Musa-Aziz, R., Chen, L. M., Pelletier, M. F., and Boron, W. F. (2009) *Proc. Natl. Acad. Sci. U.S.A.* **106,** 5406–5411